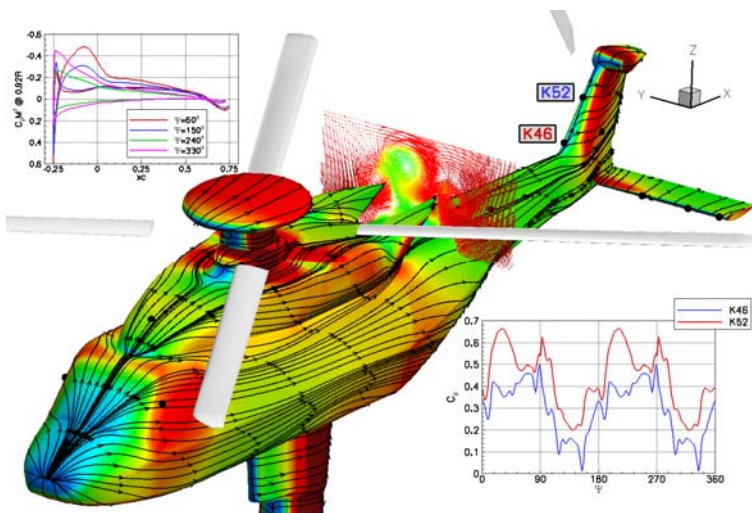## Executive summary

Aerodynamic simulation of a complete helicopter configuration

The blind test activity of the GOAHEAD project

Problem area

An important topic during helicopter development is the level of vibration in the cabin. These vibrations can be detrimental to the structure and hampering to the crew. They originate from many sources, one of them being the interaction of the (vortical) flow around the helicopter with the rotor blades and/or fuselage (for example during tail shake). These rotor-induced vibrations are passed through the rotor driving mechanism and fuselage to the cabin. High vibration levels limit the range of operational use of helicopters.

In addition, these interactions are responsible for the typical helicopter noise. Especially during low-speed descent, the interaction of the tip vortices and the rotor blades (Blade Vortex Interaction (BVI)) causes strong pressure fluctuations on the blades and associated high noise levels.

Accurate and efficient simulation of the vortex-dominated flow around helicopters still poses a major challenge. This fact impedes the routinely-based application of such simulations in the research of helicopter noise and vibration.

Description of work

A blind-test activity to evaluate and assess helicopter CFD algorithms which are used in Europe is

This report is based on a presentation held at the 33rd European Rotorcraft Forum, Kazan, Russia, September 2007.

UNCLASSIFIED

Aerodynamic simulation of a complete helicopter configuration
The blind test activity of the GOAHEAD projectThe blind test activity of the
GOAHEAD project

conducted. During the blind-test activity, simulations are performed on the GOAHEAD helicopter model for a low-speed (pitch-up) condition, a cruise condition, a high-speed tail-shake condition, a highly-loaded rotor (dynamic-stall) condition and a very high speed condition. In addition simulations are performed for the isolated fuselage.

Furthermore, the wind-tunnel test conditions are scrutinized with respect to the expected flow phenomena prior to the wind-tunnel test campaign. This test campaign is planned in January 2008 in the DNW Large Low-speed (LLF) wind tunnel.

NLR is working on the development of methods used for helicopter flow simulation. To acquire the knowledge to improve these methods efficiently, NLR participates in the EU-project 'Generation of Advanced Helicopter Experimental Aerodynamic Database for CFD code validation (GOAHEAD)'.

The main objectives of this EU-project are:
1. To enhance the aerodynamic prediction capabilities of Europe's helicopter industry with respect to complete helicopter configurations.
2. To create an experimental database for validation of 3D CFD unsteady Reynolds-averaged Navier-Stokes (URANS) methods for unsteady viscous flows including rotor dynamics for complete helicopter configurations with emphasis on phenomena like

flow separation and transition for laminar to turbulent flow.
3. To evaluate and validate Europe's most elaborate URANS solvers for the prediction of viscous flow around a complete helicopter including fluid-structure coupling.

Results and conclusions
The low-speed (pitch-up) test case should be characterized by the impingement of the rotor wake on the horizontal stabilizer. It has been shown that for the test conditions that will be used during the wind-tunnel test campaign the rotor wake is likely to impinge on the horizontal stabilizer.
Furthermore, it has been shown that for the highly-loaded (dynamic-stall) test condition the dynamic stall phenomenon is observed. However, for this test condition the required rotor driving power is too high. An alternative procedure to perform this test case has been proposed.

This blind-test activity has provided the GOAHEAD partners with an excellent means to scrutinize the wind-tunnel test conditions with respect to the expected flow phenomena prior to the wind-tunnel measurement campaign.

Based on the knowledge and experience obtained during this blind-test activity, improvements in CFD methods and procedures, for example regarding grid requirements and solver settings, will be implemented during the GOAHEAD post-test activity.

NLR-TP-2007-604

Aerodynamic simulation of a complete helicopter configuration

The blind test activity of the GOAHEAD project

O.J. Boelens, H. van der Ven, J.C. Kok, G. Barakos, M. Biava,
A. Brocklehurst, M. Costes, A. D'Alascio, M. Dietz, D. Drikakis,
J. Ekaterinaris, I. Humby, W. Khier, B. Knutzen, F. LeChuiton,
K. Pahlke, T. Renaud, T. Schwarz, R. Steijl, L. Sudre,
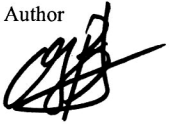L. Vigevano and B. Zhong
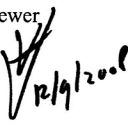
Customer	National Aerospace Laboratory NLR
Contract number	----
Owner	National Aerospace Laboratory NLR
Division	Aerospace Vehicles
Distribution	Unlimited
Classification of title	Unclassified
	December 2007

Approved by:

Author	Reviewer	Managing department
12/9/2008	12/9/2008	15/9/2008

Summary

This paper describes the blind-test CFD activity of the EU 6th Framework project GOAHEAD. This blind-test activity has been used to evaluate and assess the helicopter CFD codes which are today in use in Europe and to scrutinize the wind-tunnel test conditions with respect to the expected flow phenomena prior to the wind-tunnel test campaign. Results are presented for an isolated fuselage test case, a low-speed (pitch-up) test case, a cruise test case, a high-speed tail-shake test case and a highly-loaded rotor (dynamic-stall) test case.

Contents

4

Nomenclature

a_∞	Free-stream speed of sound [m/s]
c	Chord [m]
$C_{Mp}M^2$	Local Mach-scaled pitching moment coefficient ($=2m_p/(\rho u_i^2 cL)\cdot(u_i/a_\infty)^2)$) [-]
C_p	Pressure coefficient ($=2(p-p_\infty)/(\rho_\infty U_\infty^2)$) [-]
$C_p M^2$	Blade sectional pressure coefficient ($=2(p-p_\infty)/(\rho u_i^2)\cdot(u_i/a_\infty)^2)$) [-]
C_t	Thrust coefficient ($=2T/(\rho_\infty U_\infty^2 S)$) [-]
$C_t M^2$	Local Mach-scaled tangential force coefficient ($=2f_t/(\rho u_i^2 c)\cdot(u_i/a_\infty)^2)$) [-]
C_t/σ	Rotor loading [-]
$C_X S$	Drag coefficient ($=2F_X/(\rho_\infty U_\infty^2)$) [m^2]
F_X, F_Y, F_Z	Force components in wind-tunnel coordinate system [N]
L	Reference length (=1.0) [m]
m_p	Sectional pitching moment [Nm/m]
M_{tip}	Rotor tip Mach number [-]
$M_{tip, tr}$	Tail rotor tip Mach number [-]
M_{WT}	Wind tunnel Mach number [-]
N_b	Number of blades [-]
p	Pressure [N/m^2]
p_∞	Free-stream pressure [N/m^2]
P_{MR}	Main rotor driving power [kW]
r	Radial position along rotor blade [m]
R	Rotor radius [m]
S	Reference area (=1.0) [m^2]
T	Thrust [N]
U, V, W	Velocity components scaled with free-stream velocity U_∞ in wind-tunnel coordinate system [-]
u_i	Local blade inflow velocity ($=\Omega r + U_\infty\sin(\psi)$) [m/s]
U_∞	Free-stream velocity [m/s]
X, Y, Z	Wind-tunnel coordinates: X-axis pointing in direction of free-stream, Y-axis forming right-hand system with X- and Z-axis, Z-axis pointing upward (opposite to direction of gravity) [m]
X_f, Y_f, Z_f	Fuselage coordinates: X_f-axis pointing in direction of free-stream, Y_f-axis forming right-hand system with X_f- and Z_f-axis, Z_f-axis point upward (opposite to direction of gravity) Equal to wind-tunnel coordinates for 0° fuselage pitch attitude [m]

$\beta_0, \beta_c, \beta_s$	Flap angles: positive when blade flaps downwards (HOST [10] sign convention) [°]
$\delta_0, \delta_c, \delta_s$	Lag angles [°]
ρ_∞	Free-stream density [kg/m^3]
σ	Solidity (=$N_b c/\pi R$)[-]
τ	Non-dimensional time (=$U_\infty t/L$) [-]
θ	Fuselage pitch attitude [°]
$\theta_0, \theta_c, \theta_s$	Collective, cyclic lateral, cyclic longitudinal pitch angle: referenced to blade articulation [°]
ψ	Main rotor azimuth: zero with one of the blades parallel to the positive X-axis. Main rotor is rotating clockwise viewed from above [°]

Abbreviations

CFD	Computational Fluid Dynamics
CUN	Cranfield University
DG	Discontinuous Galerkin
DLR	Deutsches Zentrum für Luft- und Raumfahrt e.V. DLR
ECD	Eurocopter Deutschland GmbH
GOAHEAD	Generation Of Advanced Helicopter Experimental Aerodynamic Database for CFD code validation
HMB	Helicopter Multi-Block
HOST	Helicopter Overall Simulation Tool
IAG	Institut für Aerodynamik und Gasdynamik der Universität Stuttgart
MTMG	Multi-time multi-grid
NLR	Nationaal Lucht- en Ruimtevaartlaboratorium NLR
ONE	Office National d'Etudes et de Recherches Aérospatiale ONERA
PIV	Particle Image Velocimetry
POM	Politecnico di Milano
ROSITA	Rotorcraft Software Italy
SST	Shear Stress Transport
ULI	University of Liverpool

1 Introduction

The conventional helicopter is close to the limit of its performance envelope. Nowadays the emphasis in helicopter development is on making it a more efficient and environmentally friendly means of transport. Although European helicopters are among the most efficient and quiet helicopters in the world, a constant fast development in aerodynamic knowledge and capabilities regarding helicopters is required to maintain and even extend this position. Important for such a development is the availability of advanced helicopter experimental databases for CFD code validation.

In order to strengthen the competitiveness of the European aeronautic (helicopter) industries the GOAHEAD (**G**eneration **O**f **A**dvanced **H**elicopter **E**xperimental **A**erodynamic **D**atabase for CFD code validation) project [1] [2] is conducted.

This four-year research project aims at the experimental and numerical investigation of flow phenomena encountered by complex helicopter configurations. Examples of these flow phenomena are interactional effects on control surfaces and flow separation on rotor blades and fuselages. The project is partly funded by the European Union under the Integrating and Strengthening the European Research Area Programme of the 6th Framework, Contract Nr. 516074 [3].

As part of this project during the first two years a blind-test CFD activity is performed. The objectives of this blind-test activity are twofold: i) to evaluate and assess the current CFD capabilities in Europe with respect to complex helicopter configurations by means of cross-comparisons and ii) to scrutinize the wind-tunnel test conditions with respect to the expected flow phenomena prior to the wind-tunnel test campaign. Both these aspects of the blind-test activity are discussed in the present paper.

The GOAHEAD consortium consists of the four European helicopter manufacturers, i.e. Agusta S.p.a. (Italy), Westland Helicopters Ltd (United Kingdom), Eurocopter S.A.S. (France) and Eurocopter Deutschland GmbH (Germany), five aerospace research centres, i.e. Deutsches Zentrum für Luft- und Raumfahrt e.V. DLR (Germany) (coordinator of the project), Office National d'Etudes et de Recherches Aérospatiale ONERA(France), Centro Italiano Ricerche Aerospaziali S.C.P.A. CIRA (Italy), Foundation for Research and Technology FORTH (Greece) and Nationaal Lucht- en Ruimtevaartlaboratorium NLR (The Netherlands), five universities, i.e. University of Glasgow (United Kingdom), Cranfield University (United Kingdom), Politecnico di Milano (Italy), Institut für Aerodynamik und Gasdynamik der Universität Stuttgart

(Germany) and University of Liverpool (United Kingdom) and one SME, i.e. Aktiv Sensor GmbH (Germany).

The paper is set out in such a way that it provides a description of both the planned wind-tunnel test campaign and the blind-test activity of the GOAHEAD project. The wind-tunnel test campaign is discussed in section 2. Section 3 gives an overview of the blind-test activity of the GOAHEAD project. A section with conclusions completes the paper.

2 The wind-tunnel test campaign

The twelve-day wind tunnel tests campaign, which is scheduled for January 2008, will be performed in the Large Low-speed (LLF) wind tunnel of the German-Dutch wind tunnels DNW in Marknesse, The Netherlands. The 6x8x20m closed test section will be used.

The flight conditions investigated during the test campaign are:
i.   A low-speed (pitch-up) condition,
ii.   A cruise condition,
iii.   A high-speed tail-shake condition,
iv.   A highly-loaded rotor (dynamic-stall) condition, and
v.   A very high speed condition.
In addition, measurements will be performed on the GOAHEAD model with only the main and tail rotor heads mounted (isolated fuselage, no blades installed).

The wind-tunnel model used in the GOAHEAD project (see Figure 1) consists of the following parts:
- A Mach-scaled fuselage model of a modern transport helicopter: The original 1:3.881-scale model without sponsons was manufactured by NLR during the nineties. This model having a length of 4.15m was modified by removing the undercarriage nose wheels and closing the exhausts. In addition, the model was upgraded by introducing a new tail fin and tail rotor unit. Thus a complete configuration with rotating main and tail rotor was obtained.
- The 7AD rotor (including hub) consisting of four blades equipped with a swept (parabolic with anhedral) tip geometry and having a diameter of 4.2m. Note that this rotor manufactured in the eighties by Aerospatiale rotates in clockwise direction, seen from above. The zero degree azimuth position of the main rotor is defined with one of the blades pointing downstream parallel to the positive x-axis (see Figure 1).
- The two-bladed Bo105 tail rotor (diameter: 0.733m) with S102 (cambered) airfoil.

8

This so-called GOAHEAD model has been equipped with 300 static and 130 dynamic pressure sensors (100 Kulite and 30 Aktiv Sensor) on the fuselage. The main rotor has been equipped with 128 dynamic pressure sensors (Kulite), whereas 38 dynamic pressure sensors (Kulite) have been installed on the tail rotor. In addition, hot film sensors have been installed on both the fuselage (30 in total) and the main rotor (40 in total) to determine parameters associated with the boundary layer. An overview of the sensor and hot film locations on the fuselage is presented in Figure 2. Micro-tuft will be used to determine the surface stream lines and separated flow areas.

The forces experienced by the complete model as well as its components, e.g. the horizontal stabilizer or the main rotor hub, will be recorded. The blade deformations, in both bending and torsion, will be determined using the optical Stereo Pattern Recording (SPR) method of DNW-LLF and the Strain Pattern Analysis (SPA) method. Three-dimensional flow field data will be obtained using two particle image velocimetry (PIV) systems.

The data obtained during the wind-tunnel test campaign will be analyzed in detail and stored in an exhaustive, well-documented database.

3 Blind-test activitY

3.1 General description

A blind test activity has been performed using the Computational Fluid Dynamics codes which are today in use in the European helicopter industry, i.e. elsA (Eurocopter S.A.S.), FLOWer (Eurocopter Deutschland GmbH), HMB (Westland Helicopters Ltd) and ROSITA (Agusta S.p.a.), and some additional codes, which have been selected because of their promising properties regarding helicopter flow simulation, e.g. the Discontinuous Galerkin MTMG approach combined with ENSOLV (Nationaal Lucht- en Ruimtevaartlaboratorium NLR).

The following approaches regarding computational grids around the complete GOAHEAD configuration (including strut) have been used:

- *A chimera approach*. The Chimera grid was generated by Deutsches Zentrum für Luft- und Raumfahrt e.V. DLR and will be referred to as DLR Chimera grid. This Navier-Stokes grid incorporating the wind tunnel walls comprises 10 major groups, each consisting of a multi-block structured grid, with a total number of 135 blocks and 13.6 million grid points. For isolated rotor simulations only the grids around the rotor blades and a background grid have been used.

- *A sliding-grid approach*. The sliding grid was generated by the University of Liverpool and will be referred to as ULI grid. This Navier-Stokes grid consists of two parts to accommodate for the motion of the main rotor, i.e. a fuselage grid consisting of 1624 blocks and 6.4 million grid points and a rotor grid consisting of 856 blocks and 4.4 million grid points. In this grid the wind tunnel walls have not been included. This grid only has been used for the cruise test case.

- *An actuator disc approach*. This approach was adopted by Nationaal Lucht- en Ruimtevaartlaboratorium NLR. The grid will be referred to as NLR grid. Two grids were generated, i.e. a Navier-Stokes grid around the fuselage incorporating the wind-tunnel walls consisting of 3108 blocks and 10.3 million grid points and an Euler grid around the isolated rotor (without hub) consisting of 272 blocks and 0.18 million grid points. The grid around the fuselage contains actuator discs for the main and tail rotor. The input data for the main rotor actuator disc is obtained from simulations for the isolated rotor.

The test cases have been distributed among the GOAHEAD partners in such a way that most partners performed both a simulation for the isolated fuselage and a simulation for one of the other test conditions.

In the following sections the results of the GOAHEAD blind-test activity will be discussed for each of the test cases except the very high speed test case. The data shown will include surface pressure data, blade pressure data, rotor sectional moment data and field data. Figure 3 gives an overview of the sections and sensor locations that have been used during the GOAHEAD blind-test activity. These sections and sensor locations correspond to those used during the wind-tunnel test campaign.

3.2 Isolated fuselage test cases

Wind-tunnel measurements for the isolated fuselage (complete GOAHEAD model without rotor blades) will be performed for three test conditions, see Table 1. These measurements are included in the wind-tunnel test campaign to obtain reference data for the isolated fuselage.

Table 1: Overview of the isolated fuselage test conditions

Test case	Wind tunnel Mach number M_{WT} [-]	Fuselage pitch attitude θ [°]
1a	0.059	+5.0
1b	0.204	-2.0
1c	0.250	-3.5

Note that the conditions for test case 1a, 1b and 1c correspond to those of the low-speed (pitch-up) test case, the cruise and high-speed (tail-shake) test case and the very high-speed test case, respectively. In the present paper only simulations performed for test case 1b will be discussed. For this test case simulations have been performed by Cranfield University (CUN),

Eurocopter Deutschland GmbH (ECD), the Nationaal Lucht- en Ruimtevaartlaboratorium NLR (NLR) and the University of Liverpool (ULI). In all simulations the main rotor head was mounted however not rotating.

CUN and ECD used the CFD flow solver FLOWer [4] to perform this Navier-Stokes simulation on the DLR Chimera grid. CUN used the HLLC Riemann solver which has been implemented into FLOWer especially for the GOAHEAD project.

NLR employed the CFD flow solver ENSOLV [6] on the NLR grid. The actuator disc boundary conditions were set to internal face boundary conditions.

ULI performed Navier-Stokes simulations using the CFD flow solver HMB [5] on an in-house generated grid incorporating the wind tunnel walls consisting of 2226 blocks and 12.2 million grid points. All solvers were run in steady-state mode.

Figure 4 shows a comparison of the sectional surface pressure C_p at section V1 and section H3 (see Figure 3). Note that for section V1 no data is shown for the bottom of the cabin. Despite the different computational grids, numerical methods, turbulence models, etc. used for these simulations by the GOAHEAD partners the agreement in sectional surface pressure is generally good. Note that for $2.7 < X_f < 3.5$ two sets of solutions can be observed in section H3, one set containing data of CUN and ECD and one set containing data of NLR and ULI. Further differences occur in rear door region and in the region on the fuselage behind the hub.

In Figure 5 pressure sensor data is shown for the sensor locations depicted in Figure 3. Neighboring sensors are grouped together. Here also the differences in the rear door region can be observed.

Finally, Figure 6 shows the velocity vector field for plane S6. This plane corresponds to section S6 shown in Figure 3. Note that the plane shown is approximately the PIV window that will be used during the wind tunnel campaign. The vortices originating from the engine exhausts are clearly visible. The vortex core location varies slightly for the different solutions. Note also that CUN and NLR have symmetric solutions, while ECD and ULI have asymmetric solutions.

3.3 Low-speed (pitch-up) test case

Pitch-up is a low speed aerodynamic interference phenomenon which occurs during transition from hover to a medium cruise speed. The objective of this simulation was to verify whether for the selected wind tunnel test condition the rotor wake impinges on the horizontal stabilizer, which is characteristic for the pitch-up phenomenon. Table 2 shows the test condition considered. Based on this test condition, initial settings for blade control angles have been calculated using the aeromechanical code HOST [10] by Eurocopter S.A.S.

For this test case a simulation for the complete configuration including the tail rotor has been performed by the Institut für Aerodynamik und Gasdynamik der Universität Stuttgart (IAG).

Table 2: Overview of the low-speed (pitch-up) test conditions

Test case	Wind tunnel Mach number M_{WT} [-]	Fuselage pitch attitude θ [°]	Rotor loading C_t/σ [-]	Rotor tip Mach number M_{tip} [-]	Tail rotor tip Mach number $M_{tip, tr}$ [-]	Drag $C_X S$ [m^2]
2	0.059	+5.0	0.071	0.617	0.566	0.176

IAG used the CFD flow solver FLOWer [4] to perform this Navier-Stokes simulation on the DLR Chimera grid. The flow solver was weakly coupled with the aeromechanical code HOST, see also section 3.5. Elastic blade deformations were incorporated in both FLOWer and HOST. The collective and cyclic pitch angles were used as free variables to trim the rotor to the prescribed mean rotor forces. For the present simulation, starting from the initial settings five trim iterations were needed to obtain converged control angles.

The resulting blade control angles referenced to the blade articulation are summarized in Table 3. The flap angle is positive when the blade flaps downwards (following the sign convention used in HOST). The tail rotor has a constant pitch attitude of 8.99°.

Table 3: Blade control angles referenced to the blade articulation for the low-speed (pitch-up) test case. The flap angle is positive when the blade flaps downwards (HOST sign convention).

	θ_0[°]	θ_c[°]	θ_s[°]	β_0[°]	β_c[°]	β_s[°]	δ_0[°]	δ_s[°]	δ_s[°]
IAG	9.76	1.76	-2.56	-1.96	-0.76	1.29	0.74	0.20	-0.02

Figure 7 shows for three azimuthal positions, i.e. ψ=0°, 30° and 60°, the out-of-plane (y-direction) vorticity component $\omega_y L/U_\infty$ in plane V3. This plane corresponds to section V3 shown in Figure 3. Note that the plane shown is approximately the PIV window that will be used during the wind tunnel campaign. This figure shows the vortex generated by the passing main rotor blade as well as the evolution of this vortex in time. It is evident from this figure that for the selected test condition the rotor wake is likely to impinge on the horizontal stabilizer.

3.4 Cruise and high-speed (tail-shake) test case

Tail shake is an aerodynamic phenomenon resulting from the interaction of the rotor hub wake with the tail boom and vertical tail. This interaction results in a low frequency vibration of the tail boom. During the wind-tunnel test campaign the cruise and high-speed (tail-shake) test conditions only differ with respect to fuselage pitch attitude θ. Whereas for the cruise test

condition the fuselage pitch attitude is fixed to -2.0°, the pitch attitude for the high-speed (tail-shake) test case is altered by rotating the model forward until tail-shake is encountered. Prior to the wind-tunnel test campaign the pitch attitude is therefore unknown for the high-speed (tail-shake) test case. A fixed pitch attitude of -2.0° has been adopted during the blind-test activity. Table 4 shows the test condition considered. Based on these test conditions initial settings for blade trimming angles have been calculated using the aeromechanical code HOST [10] by Eurocopter S.A.S.

Table 4: Overview of the cruise and high speed (tail-shake) test conditions

Test case	Wind tunnel Mach number M_{WT} [-]	Fuselage pitch attitude θ [°]	Rotor loading C_t/σ [-]	Rotor tip Mach number M_{tip} [-]	Tail rotor tip Mach number $M_{tip,\,tr}$ [-]	Drag C_XS [m²]
3/4	0.204	-2.0	0.071	0.617	0.566	0.185

For this test case simulations have been performed by Deutsches Zentrum für Luft- und Raumfahrt e.V. (DLR), Nationaal Lucht- en Ruimtevaartlaboratorium NLR (NLR), Politecnico di Milano (POM) and the University of Liverpool (ULI).

DLR used the CFD flow solver FLOWer [4] to perform this Navier-Stokes simulation on the DLR Chimera grid. The trimming approach is similar the one described for IAG in section 3.3. Elastic blade deformations were incorporated.

At NLR first an Euler simulation including elastic blade deformation was performed using the Discontinuous Galerkin MTMG approach [7] on the isolated rotor grid. The rotor was trimmed to the predefined thrust and zero rotor moments by automatically modifying the pitch control angles. Next, a steady Navier-Stokes simulation was performed employing the CFD flow solver ENSOLV [6] on the grid around the fuselage. The input data for the main rotor actuator disc was obtained from the isolated rotor simulation.

At POM the CFD flow solver ROSITA [8] has been used to perform this Navier-Stokes simulation on a modified version of the DLR Chimera grid. POM employed the final blade control angles obtained by DLR.

ULI used the CFD flow solver HMB [5] to perform the Navier-Stokes simulations on the ULI grid. Note that this method employs a recently-developed sliding-grid approach to include the rotor motion in the simulation [9]. The blade control angles used by ULI are those calculated using the aeromechanical code HOST by Eurocopter S.A.S.

The resulting blade control angles referenced to the blade articulation are summarized in Table 5. The flap angle is positive when the blade flaps downwards (following the sign convention used in HOST). The tail rotor was modeled in both the DLR and NLR simulations. The blade control angles used by DLR for the tail rotor are: θ_0=6.63°, β_c=3.40° and β_s=-2.50°. In the NLR simulation the tail rotor was modeled using an actuator disc with constant thrust.

Table 5: Blade control angles referenced to the blade articulation for the cruise and high speed (tail shake) test case. The flap angle is positive when the blade flaps downwards (HOST sign convention).

	θ_0[°]	θ_c[°]	θ_s[°]	β_0[°]	β_c[°]	β_s[°]	δ_0[°]	δ_s[°]	δ_s[°]
DLR/POM	12.85	1.08	-6.58	-1.95	-0.19	1.13	-0.31	0.21	-0.09
NLR	12.73	2.10	-6.00	0.00	0.00	0.00	0.00	0.00	0.00
ULI	12.40	2.27	-6.98	-2.64	-0.56	-0.28	0.00	0.00	0.00

Pressure sensor data for the sensor locations depicted in Figure 3 is shown in Figure 8. Neighboring sensors are grouped together. Due to the steady approach of the NLR simulation around the fuselage constant signals are obtained. Note also the high-frequency effect observed by pressure sensor K57 on the vertical tail due to the presence of the tail rotor in the DLR simulation.

This figure gives an indication of the pressure sensor data to be expected in the wind-tunnel test campaign. By comparing this figure with Figure 5 the effect of incorporating the main rotor can be observed.

Figure 9 shows the sectional surface pressure distribution C_p at r/R=0.81. Hot film sensors will be used during the wind-tunnel test campaign to obtain blade surface pressure data in a number of sections including this one. Keeping in mind the different approaches used for these simulations by the GOAHEAD partners the agreement between the solutions is good.

Finally, Figure 10 shows the velocity vector field for plane S6. Note that this plane corresponds to the plane shown in Figure 6 for the isolated fuselage test case having the same wind-tunnel test conditions. Due to the steady approach of the NLR simulation around the fuselage a steady vector field was obtained. The variation with respect to main rotor azimuth angle can be observed in the DLR solution. Once more the vortices originating from the engine exhausts are clearly visible. However, additional vortical structures are visible, for example at (Y,Z)=(-0.05,1.02) for the DLR solution at 60° azimuth angle and at (Y,Z)=(0.07,1.05) for the NLR solution. For a different pitch attitude these vortical structures may trigger the tail shake phenomenon.

3.5 Highly-loaded rotor (dynamic-stall) test case

For this test case simulations for the isolated 7AD rotor have been performed by Eurocopter
Deutschland GmbH (ECD) and the University of Liverpool (ULI). The objective of these
simulations was to identify a wind tunnel test condition with the highest possibility of observing
the dynamic-stall phenomenon. This condition should, however, lie within the limits of the
wind-tunnel test environment, in particular the limits regarding the required rotor driving power.
Table 6 shows the test conditions considered.

Table 6: Overview of the highly loaded rotor (dynamic stall) test conditions

Test case	Wind tunnel Mach number M_{WT} [-]	Fuselage pitch attitude θ [°]	Rotor loading C_t/σ [-]	Rotor tip Mach number M_{tip} [-]	Drag $C_X S$ [m^2]
5a	0.194	-2.0	0.110	0.617	0.185
5b	0.259	-7.0	0.096	0.617	0.215
5c	0.249	-7.0	0.096	0.617	0.100

ECD performed Navier-Stokes simulations on the DLR Chimera grid using the CFD flow solver
FLOWer [4] weakly coupled with the aeromechanical code HOST [10]. HOST uses the
aerodynamic loads provided by FLOWer to correct its internal 2D aerodynamics and
subsequently retrims the rotor. The blade dynamic response is introduced in FLOWer in order to
obtain updated aerodynamic loads. The test conditions in Table 6 have been used as trim
objective for the HOST calculations carried out during this weak coupling procedure. For the
present simulations, starting from the initial settings four trim iterations were needed to obtain
converged control angles.

ULI used the CFD flow solver HMB [5] to perform the Navier-Stokes simulations on an in-
house generated isolated rotor grid consisting of 1000 blocks and 7.0 million grid points. The
blade control angles used by ULI were obtained from previous wind-tunnel tests for the isolated
7AD rotor. The blade control angles have been modified by using the flap-pitch equivalence to
remove the harmonic flapping and by adjusting the shaft tilt angle to remove the 'cosine
flapping' coefficient.

The resulting blade control angles referenced to the blade articulation are summarized in Table
7. The flap angle is positive when the blade flaps downwards (following the sign convention
used in HOST).

Table 7: Blade control angles referenced to the blade articulation for the highly loaded rotor (dynamic stall) test case. The flap angle is positive when the blade flaps downwards (HOST sign convention).

	$\theta_0[°]$	$\theta_c[°]$	$\theta_s[°]$	$\beta_0[°]$	$\beta_c[°]$	$\beta_s[°]$	$\delta_0[°]$	$\delta_s[°]$	$\delta_s[°]$
ECD 5a	15.66	1.98	-6.20	-3.00	2.87	0.94	-1.09	0.27	-0.43
ECD 5b	20.72	2.87	-10.50	-2.55	3.12	1.36	-3.92	0.39	-0.68
ECD 5c	17.84	1.23	-5.66	-2.57	6.07	1.06	-1.97	0.19	0.18
ULI 5a	14.39	2.88	-9.92	-2.49	0.00	0.00	0.00	0.00	0.00

Figure 11 shows for three radial positions on the blade, i.e. r/R=0.700, 0.820 and 0.915, a comparison of the local Mach-scaled pitching moment coefficient $C_{Mp}M^2$ as function of the azimuth angle ψ. The corresponding distribution of the local Mach-scaled pitching moment coefficient $C_{Mp}M^2$ on the rotor disc is shown in Figure 12.

From these figures it is clear that the dynamic stall phenomenon appears in test case 5b. The impulsive change of the local Mach-scaled pitching moment coefficient $C_{Mp}M^2$ on the retreating side of the rotor caused by flow separation on the blade is present at the radial position r/R=0.820 for azimuth angles between approximately 210° and 300°. For the radial position r/R=0.915, this behavior is present for azimuth angles between approximately 240° and 360°. The flow separation region is thus shifting outward for increasing azimuth angle. Both test case 5a and test case 5c do not show such a clear stall region.

In Table 8 an estimation of the required rotor driving power for each test case is shown. The required rotor driving power for test case 5b was found to be significantly higher than that required for the other two test cases.

Although test case 5b seems most suited for a dynamic stall wind tunnel measurement campaign, the required rotor driving power is considered too high for the engine integrated into the model. In addition the control angles for test case 5b were found to be very high, see Table 7. Therefore to ensure the safety of the rotor in such a highly loaded situation, it was recommended to start with the test conditions of test case 5c during the wind tunnel measurement campaign, subsequently incline the tip path plane forward until the dynamic stall phenomenon is encountered and perform the measurements at these conditions.

Table 8: Estimation of the required rotor driving power

Test case	P_{MR} [kW]
5a	103
5b	189
5c	130

4 Concluding remarks

In the framework of the EU 6th Framework project GOAHEAD, a blind-test CFD activity has been performed.

This blind-test activity has provided the GOAHEAD partners with an excellent means to evaluate and assess the helicopter CFD codes which are today in use in Europe and to scrutinize the wind-tunnel test conditions with respect to the expected flow phenomena prior to the wind-tunnel measurement campaign.

During this blind-test activity, simulations have been performed on the GOAHEAD model for a low-speed (pitch-up) condition, a cruise condition, a high-speed tail-shake condition, a highly-load rotor (dynamic-stall) condition and a very high speed condition. In addition simulations have been performed for the isolated fuselage. Results of this blind-test activity have been presented in this paper.

It has been shown that for the low-speed (pitch-up) test case the rotor wake is likely to impinge on the horizontal stabilizer for the test conditions that will be used during the wind-tunnel test campaign. Furthermore, it has been shown that for the highly-loaded (dynamic-stall) test condition with dynamic stall the required rotor driving power is too high. An alternative procedure to perform this test case has been proposed.

Based on the knowledge and experience obtained during this blind-test activity, improvements in CFD methods and procedures, for example regarding grid requirements and solver settings, will be implemented during the GOAHEAD post-test activity.

Acknowledgments

References

[1]   http://www.dlr.de/as/en/desktopdefault.aspx/tabid-3384/5247_read-7664 [cited October 2007].

[2]   K. Pahlke, *"The GOAHEAD project"*, 33rd European Rotorcraft Forum, Kazan, Russia, 2007.

[3]   Deutsches Zentrum für Luft- und Raumfahrt e.V. DLR, *"Generation of Advanced Helicopter Experimental Aerodynamic Database for CFD code validation – GOAHEAD – Contract Nr. 516074: Annex I – Description of Work"*, November 2005.

[4]   K. Becker, N. Kroll, C.C. Rossow and F. Thiele, *"The MEGAFLOW project"*, Aerospace Sci. Technol. 4, 2000, pp. 223-237.

[5]   R.Steijl, G. Barakos and K. Badcock, *"A framework for CFD analysis of rotors in hover and forward flight"*, Int. J. for Num. Meth. In Fluids, vol. 51, 2006, pp. 819-847.

[6]   *"ENFLOW: A computer code system for accurate simulation of three-dimensional flows"*, URL: http://www.nlr.nl/documents/flyers/f222-01.pdf [cited October 2007].

[7]   H. van der Ven and O.J. Boelens, *"A framework for aeroelastic simulations of trimmed rotor systems in forward flight"*, 30th European Rotorcraft Forum, Marseille, France, 2004, also available as NLR-TP-2004-409.

[8]   M. Biava, J.-C. Boniface and L. Vigevano, *"Influence of wind-tunnel walls in helicopter aerodynamcs predictions"*, 31st European Rotorcraft Forum, Florence, Italy, 2005.

[9]   R. Steijl and G. Barakos, "CFD analysis of rotor-fuselage interactional aerodynamics", AIAA-2007-1278, 2007.

[10] B. Benoit, A.M. Dequin, K.Kampa, W. von Gruenhagen, P.M. Basset and B. Gimonet., *"HOST, a general helicopter simulation tool for Germany and France"*, In *American Helicopter Society 56th Annual Forum*, Virginia Beach, Virginia, USA, 2 - 4 May 2000.
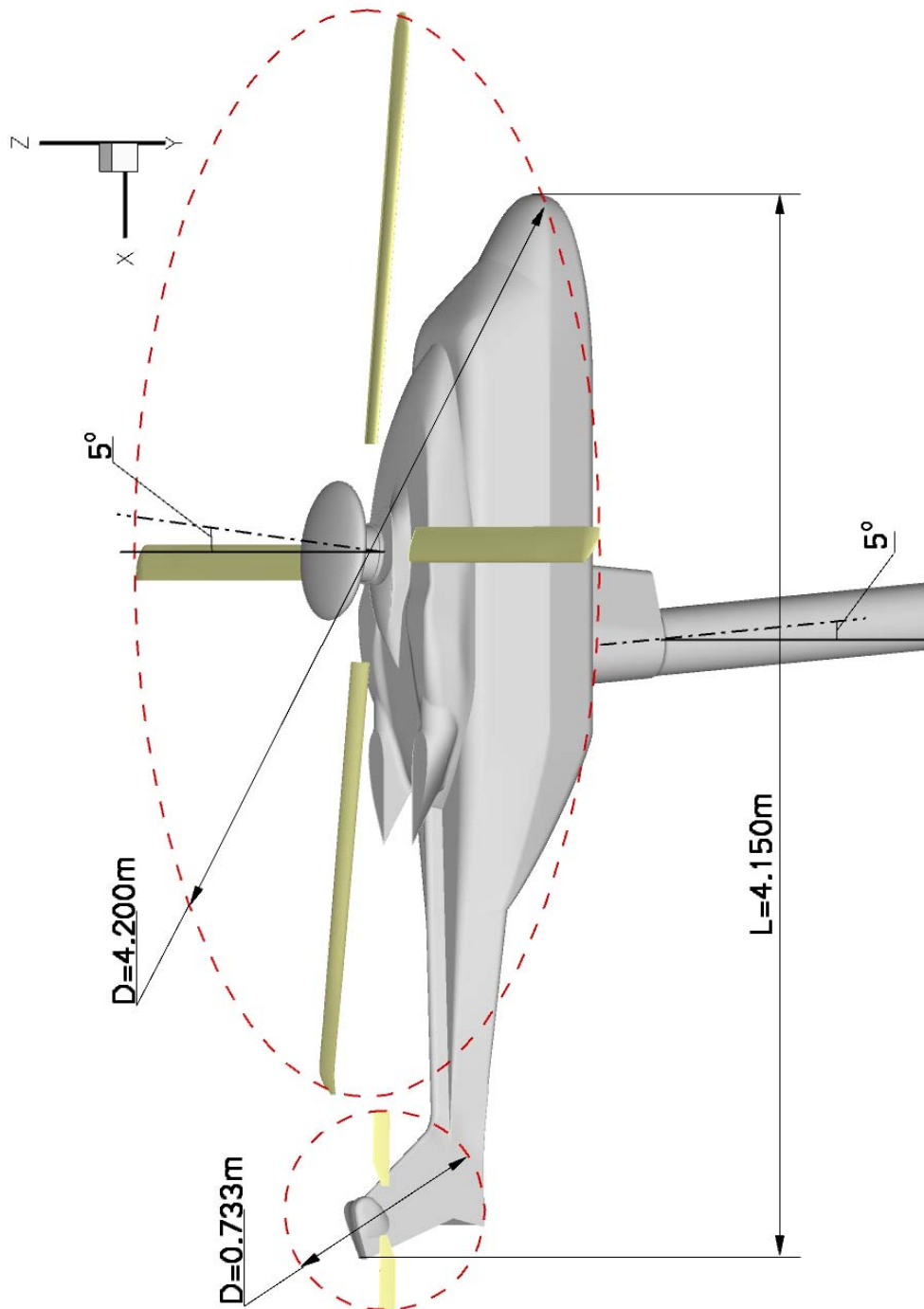
Figure 1: Overview of the GOAHEAD wind tunnel model including some geometrical details at a fuselage pitch attitude of zero degrees
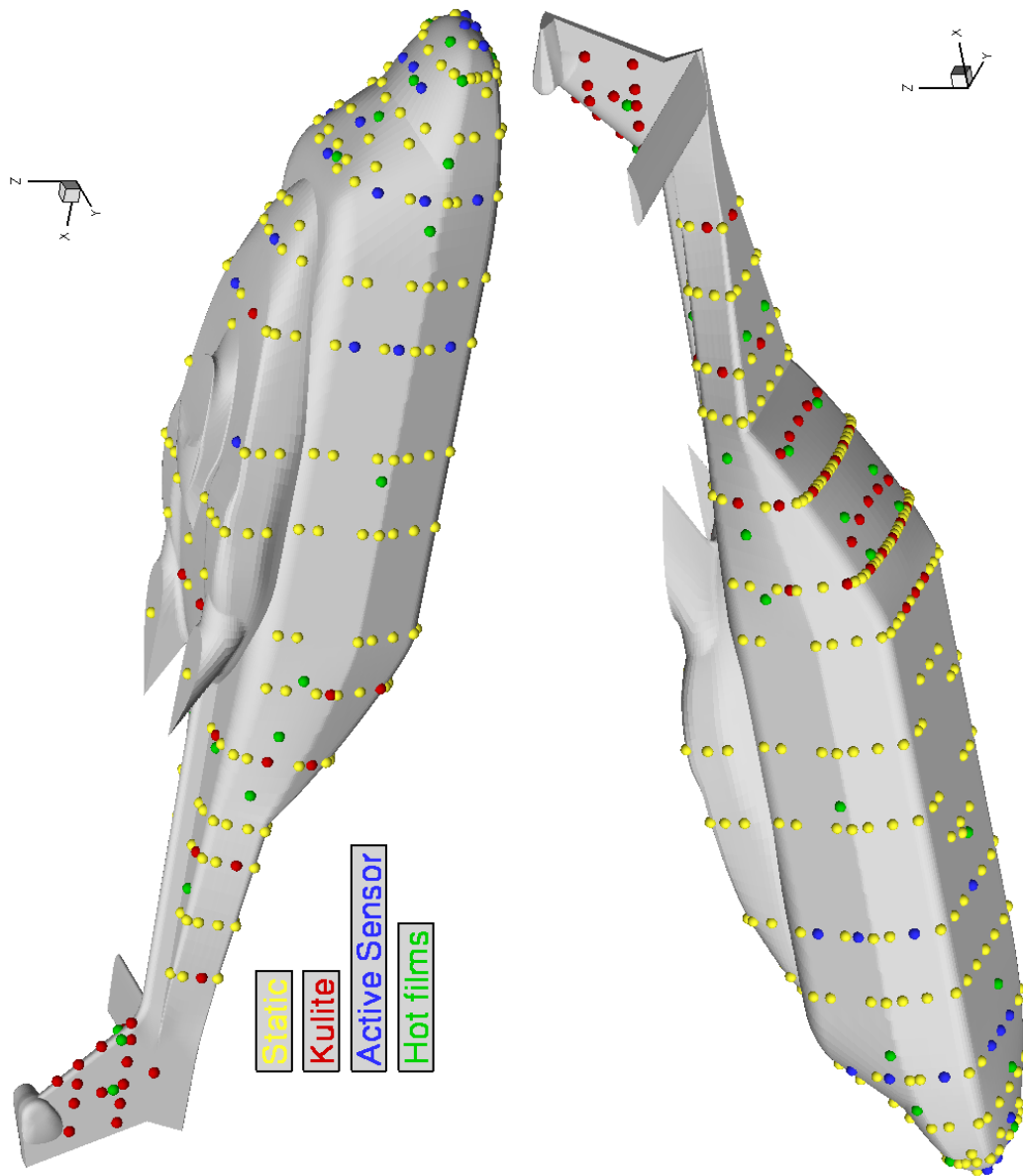
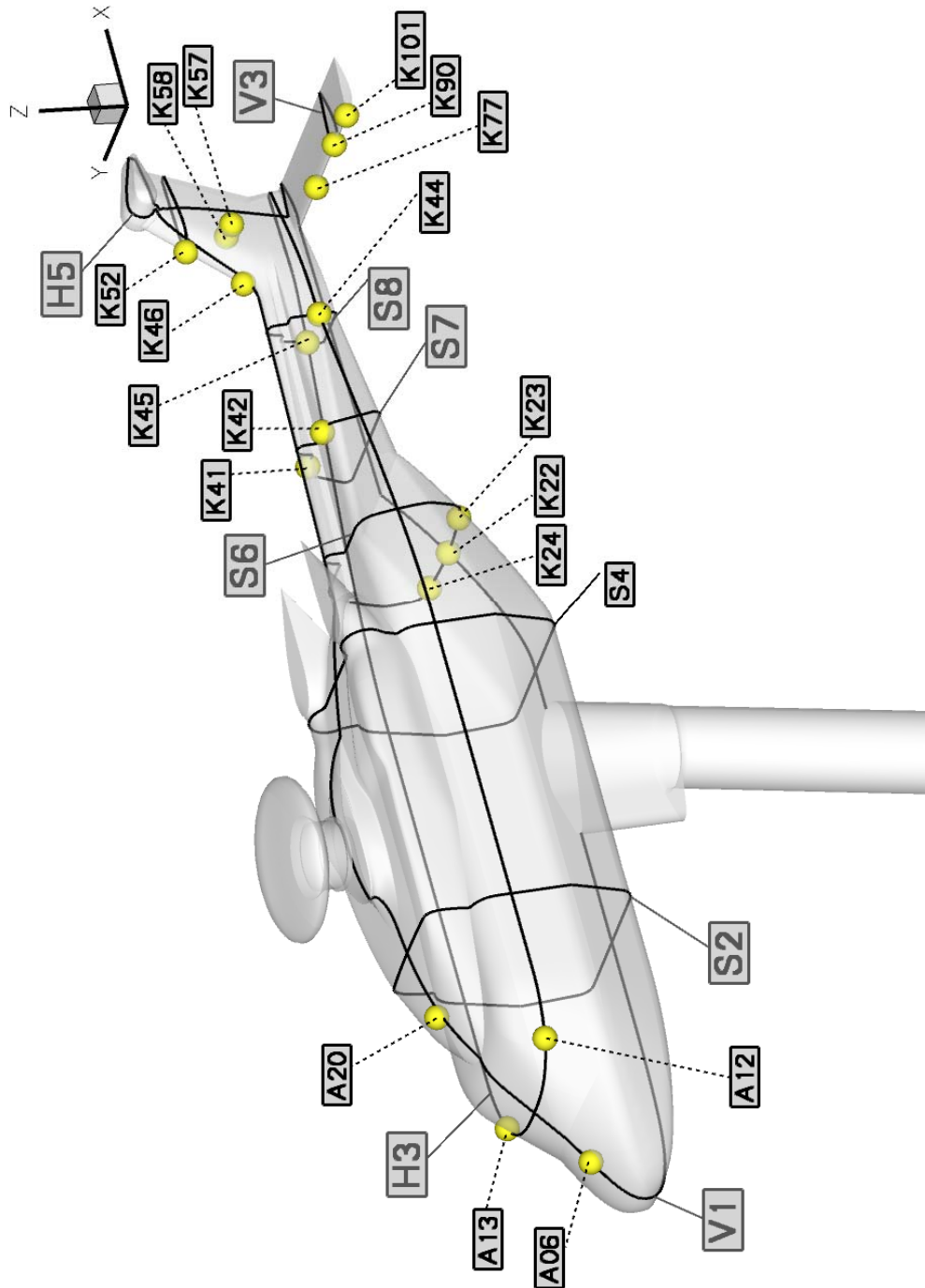Figure 2: Overview of the sensor and hot film locations on the fuselage.

Figure 3: Overview of sections and sensor locations used during the GOAHEAD blind-test activity. Note that particle image velocimetry planes S6 and V3 correspond to the sections S6 and V3.
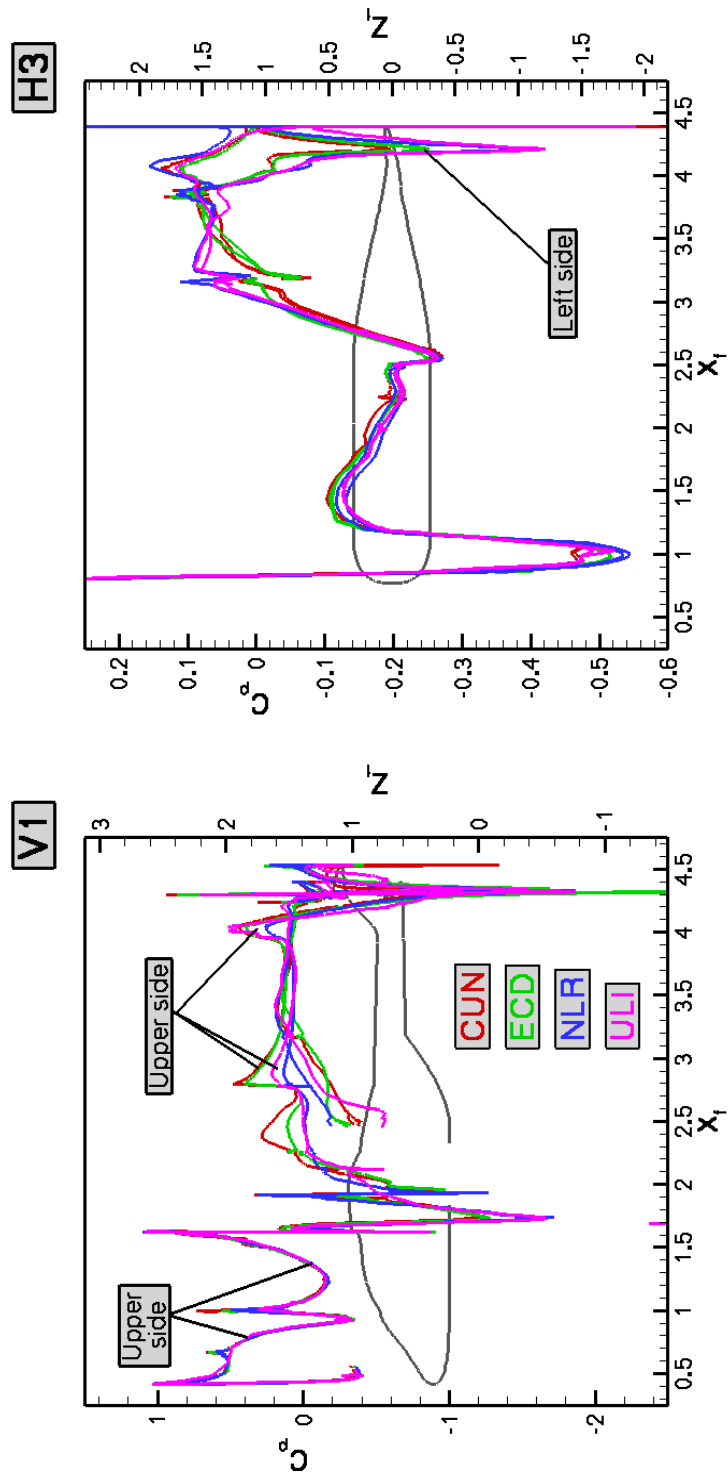
Figure 4: Sectional surface pressure C_p at section V1 (left figure; no data shown for the bottom of the cabin) and section H3 (right figure) for the isolated fuselage test case (M_{WT}=0.204, θ=-2.0°).
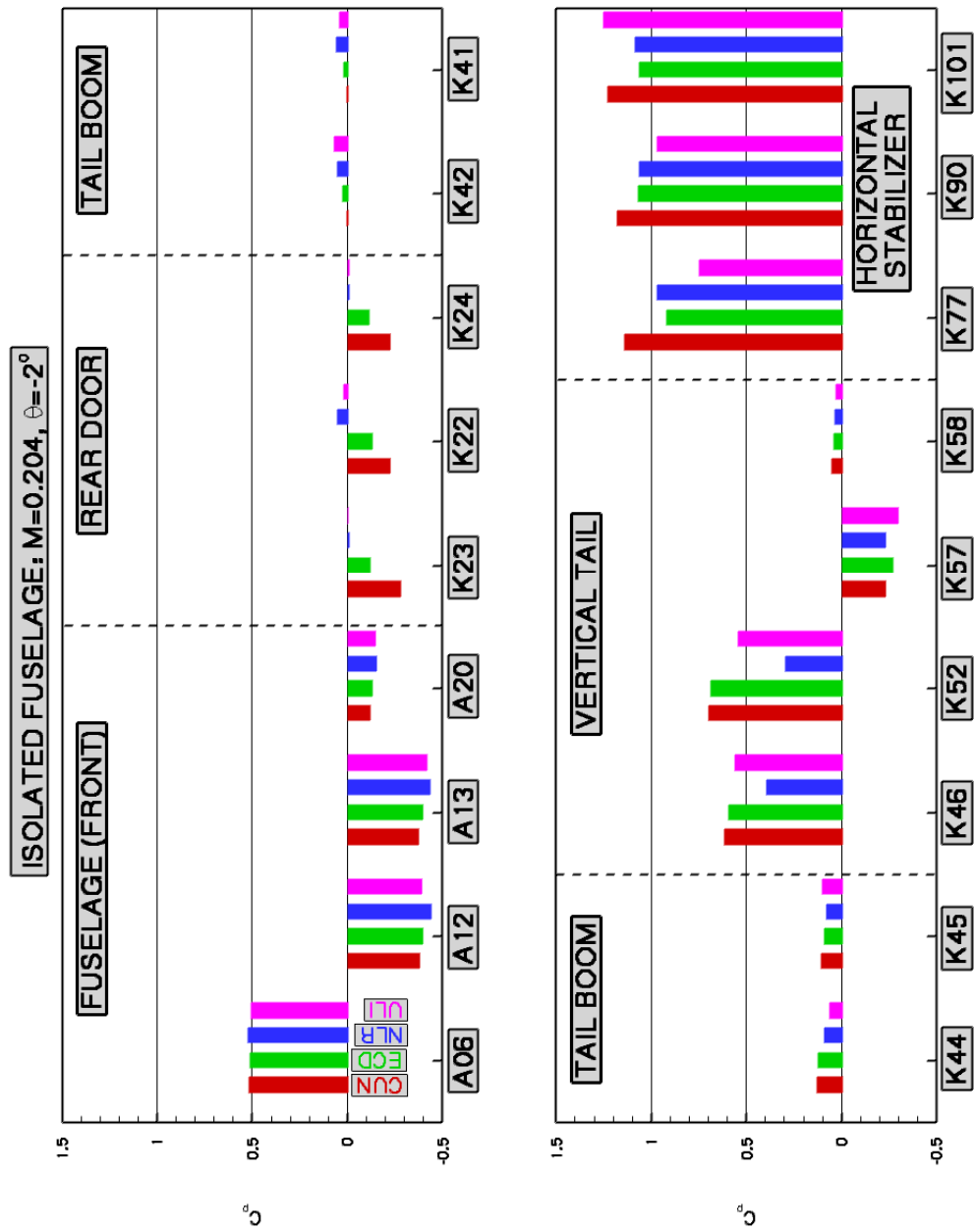
Figure 5: Pressure sensor data (C_p) for the isolated fuselage test case (M_{WT}=0.204, θ=-2.0°).
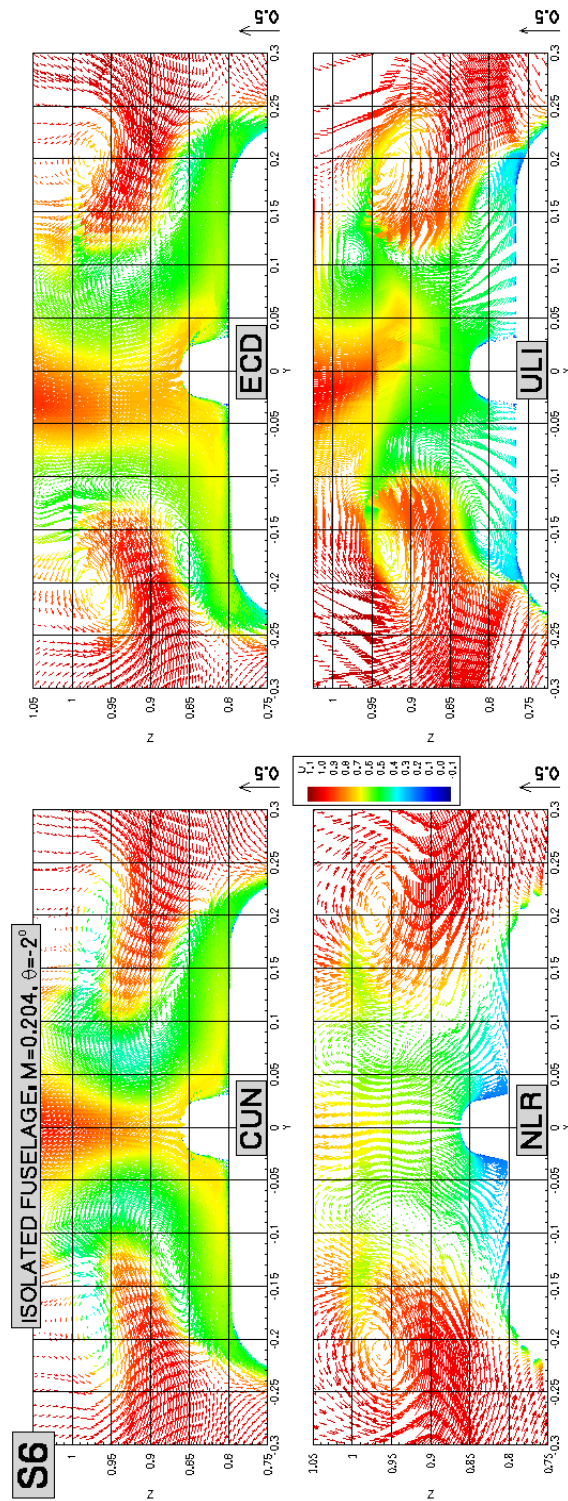
Figure 6: Velocity vector field for plane S6, i.e. a plane intersecting the fuselage at section S6, for the isolated fuselage test case (M_{WT}=0.204, θ=-2.0°). The 2-D velocity vectors (V,W) are coloured with the out-of-plane velocity component (U).

25
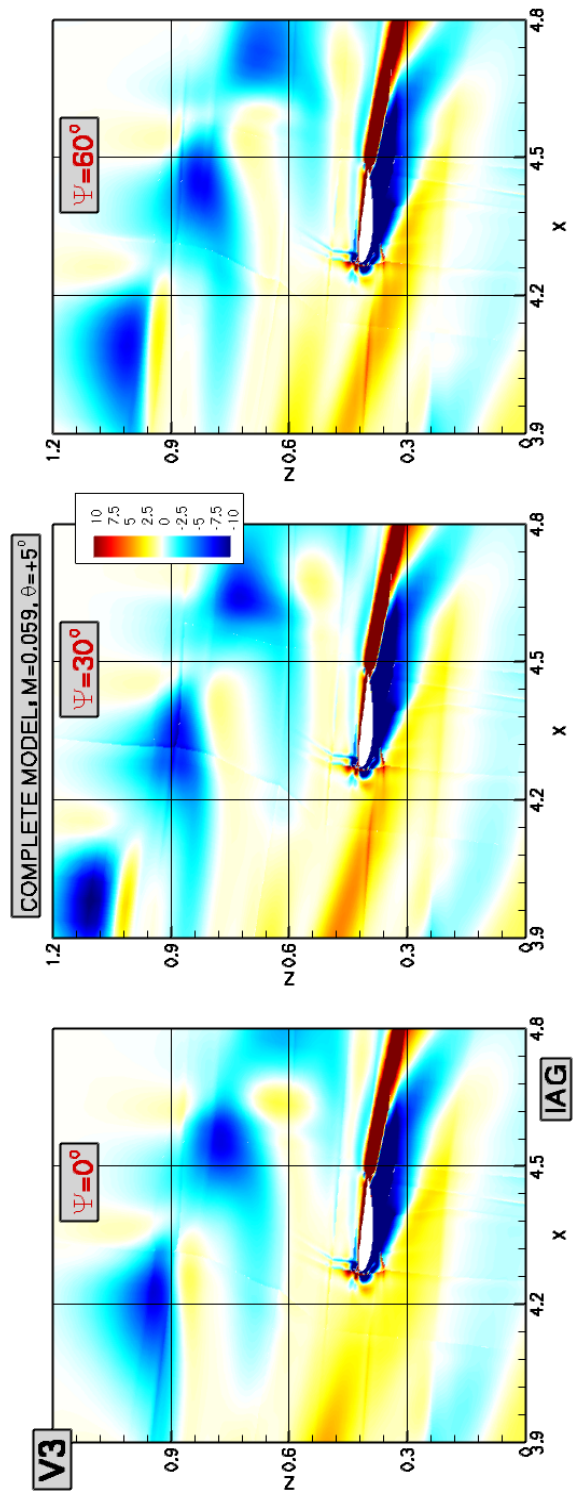
Figure 7: Out-of-plane (y-direction) vorticity component $\omega_y L/U_\infty$ for plane V3, i.e. a plane intersecting the horizontal stabilizer at section V3, for three azimuthal positions of the main rotor for the low-speed (pitch-up) test case.
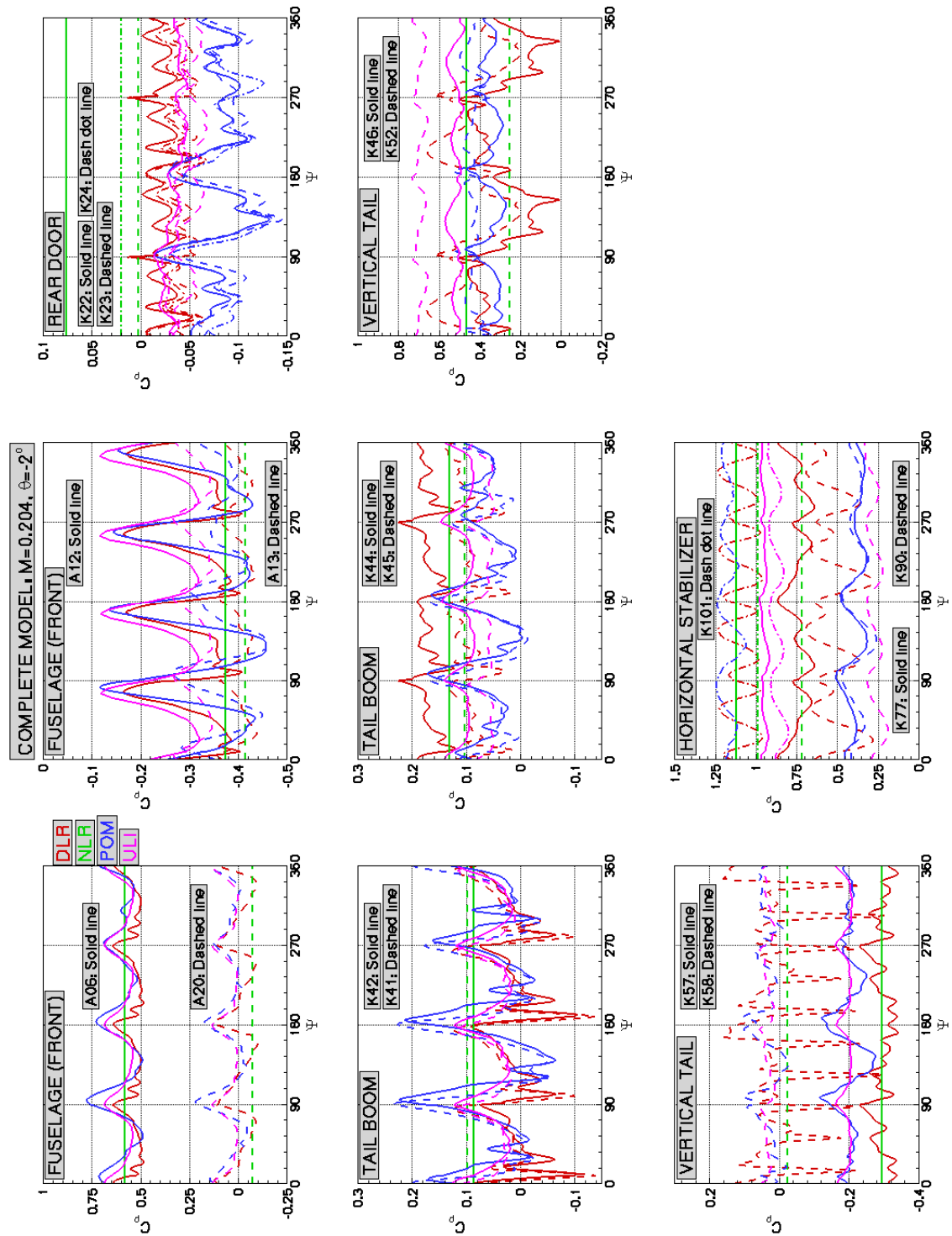
Figure 8: Pressure sensor data (C_p) for the cruise and high-speed (tail-shake) test case.
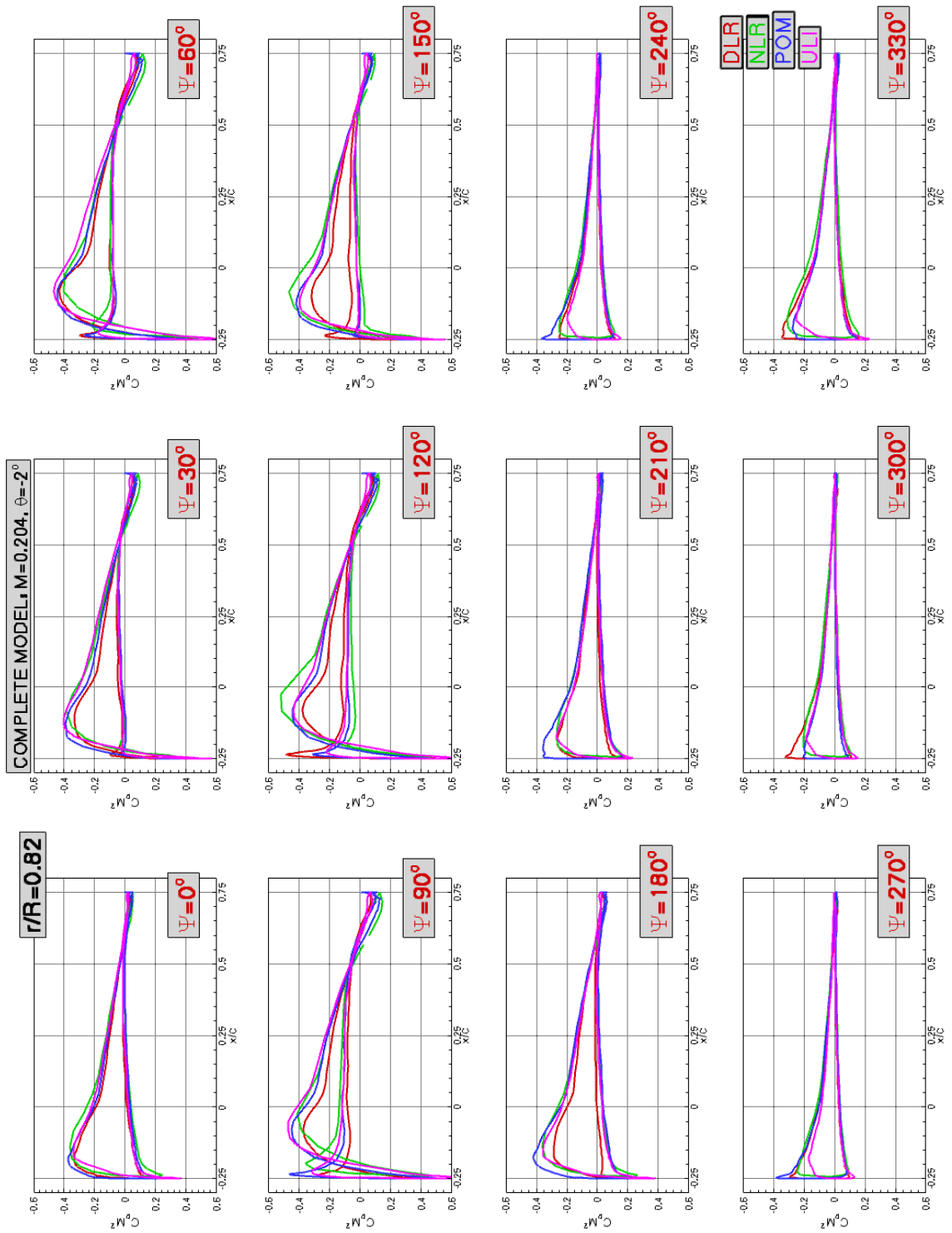
Figure 9: Sectional surface pressure data (C_p) for the main rotor at r/R=0.81 for the cruise and high-speed (tail-shake) test case. Solutions are shown at 30°azimuthal intervals.
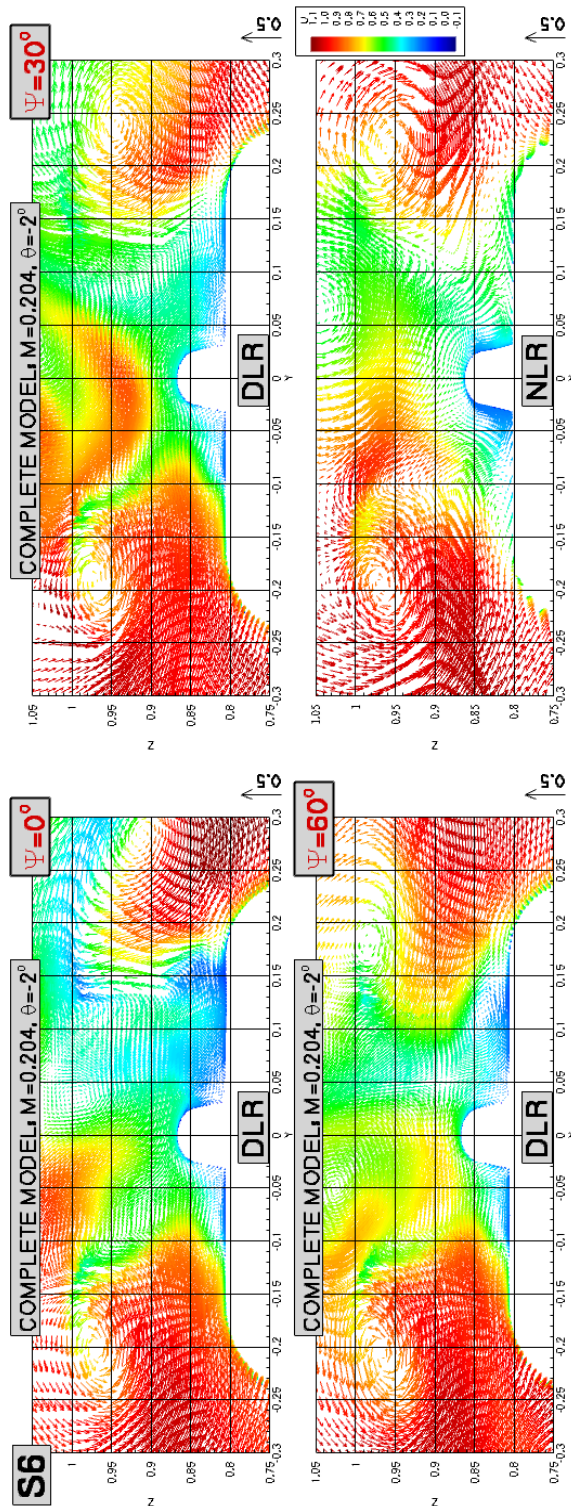
Figure 10: Velocity vector field for plane S6, i.e. a plane intersecting the fuselage at section S6, for the cruise and high-speed tail-shake test case. The 2-D velocity vectors (V,W) are coloured with the out-of-plane velocity component (U). DLR solutions are shown for 0°, 30° and 60° main rotor azimuth.
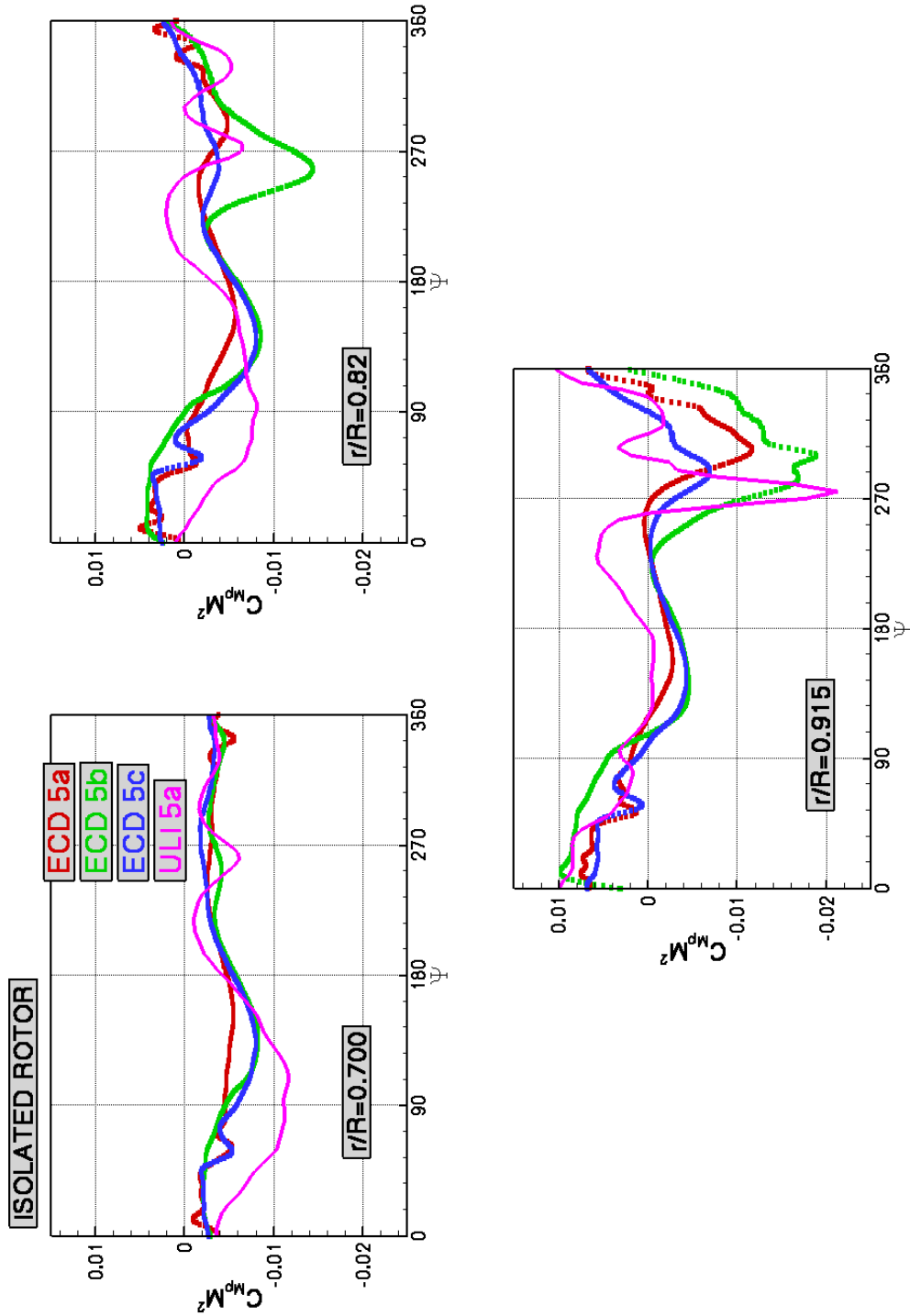
Figure 11: $C_{Mp}M^2$ (local Mach-scaled pitching moment coefficient) for three radial positions (r/R=0.700, 0.820 and 0.915) as function of the blade azimuth
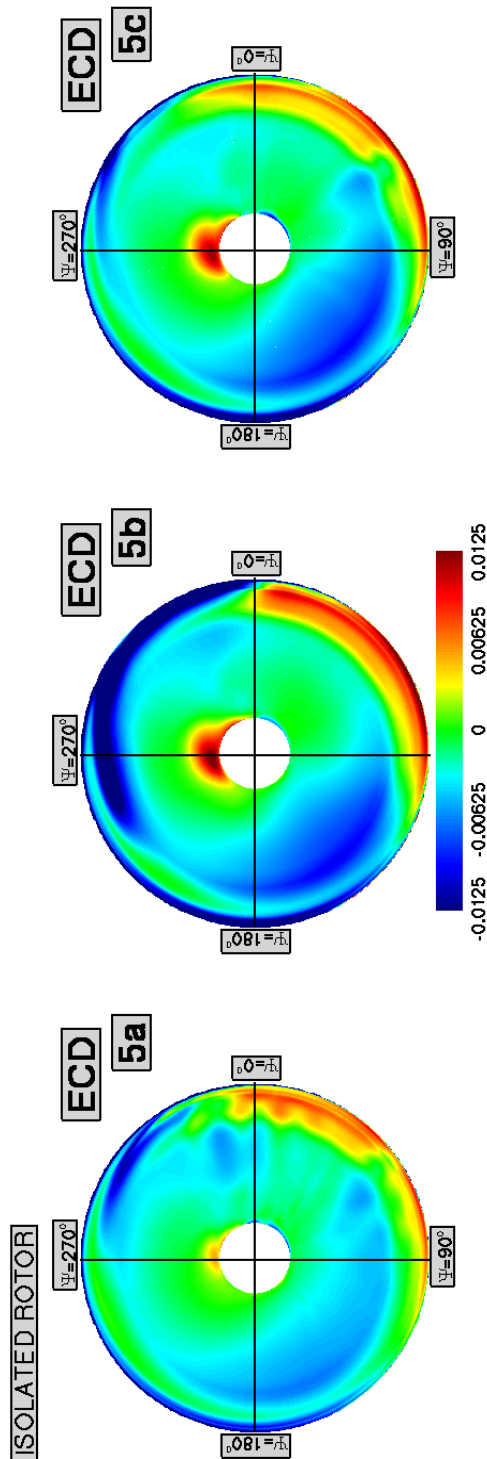
Figure 12: $C_{Mp}M^2$ (local Mach-scaled pitching moment coefficient) as function of the radial position and the blade azimuth angle

31